Journal of Ceramic Processing Research. Vol. 6, No. 3, pp. 266~270 (2005)

J O U R N A L O F
Ceramic
Processing Research

A fracture model and prediction of mechanical behavior in Si_3N_4 laminate composites

Dong-Woo Shin* and Hai Guo
Ceramic Matrix Composites (CMCs) Lab., Division of Advanced Materials Science and Engineering, Engineering Research Institute, Gyeongsang National Univesity, Jinju, Gyeongnam 660-701, Korea

A fracture model is proposed to describe the fracture behavior of laminated ceramic composites. The results reveal that the actual energy absorbed, W_{act}, by crack propagation is more suitable than work-of-fracture to calculate the toughness of composites. Fracture toughness of composites is obtained using the proposed model taking actual energy absorption into account. The predicted load-displacement curve matches with the experimental results. The results based on the proposed model regarding the influence of layer thickness and the interfacial bonding strength on fracture toughness hold valid with the calculated range.

Key words: Si_3N_4 Laminate Composite, fracture model, fracture toughness, actual energy absorption.

Introduction

Natural biomaterials such as nacre, bamboo, and wood have a composite structure and exhibit good mechanical properties [1-3]. Nacre has a typical laminated structure and because of this uniqueness the work of fracture is two orders of magnitude higher than that of a conventional aragonite crystal.

Recently, Liu and Hsu described the fracture behavior of Si_3N_4/BN laminated ceramics [4]. Modeling of crack propagation based on the energy of interfacial cracking in laminated ceramics has also been reported [5-6]. Phillips et al. [5-6] analyzed the mechanical behavior of laminated ceramics and proposed a model of a laminated ceramic to predict the energy process under bending. In this article a modified model is set up to analyze the fracture behavior of Si_3N_4/BN laminated ceramics to predict the mechanical properties of laminated ceramics.

Experimental Procedures

Si_3N_4/BN-Al_2O_3 laminated ceramics were made to mimic the structure of nacre. Si_3N_4 single crystals and SiC whisker reinforcements were used to act as secondary toughening phase. BN was selected as the separation layer in which Al_2O_3 is added to adjust the interfacial strength. A typical micrograph of a laminated Si_3N_4 ceramic is given in Figure 1.

β-Si_3N_4 seeds used in this study were prepared by heating a powder mixture of 90 wt% α-Si_3N_4, 7 wt% Y_2O_3, and 3 wt% Al_2O_3 at 1850 °C for 1.5 h under a nitrogen pressure of 0.5 MPa [4]. The synthesized seeds consisted of rodlike β-Si_3N_4 single crystals with a mean diameter of 0.5 mm and a mean length of 4.0 mm.

Sheets were formed using 12 wt% poly (vinyl) alcohol (PVA) as the organic binder, 3 wt% glycerol as the plasticising agent, and a ball-milled mixture of α-Si_3N_4 (Founder Corporation, Beijing, China), 7 wt% Y_2O_3 (purity > 99.9% Hokke Chemicals, Tokyo, Japan), 3 wt% Al_2O_3 (purity > 99.9%), and 15 wt% SiC whiskers or 3 wt% β-Si_3N_4 seeds. The sheets were formed first through coarse compact rollers and then through fine compact rollers. The green sheet was 0.2 mm thick. The sheets were cut and coated with an interfacial slurry consisting of 75 wt% BN and 25 wt% Al_2O_3 slurry. The green sheets were cut (32 mm × 38 mm) and stacked in a particular order in a graphite die.

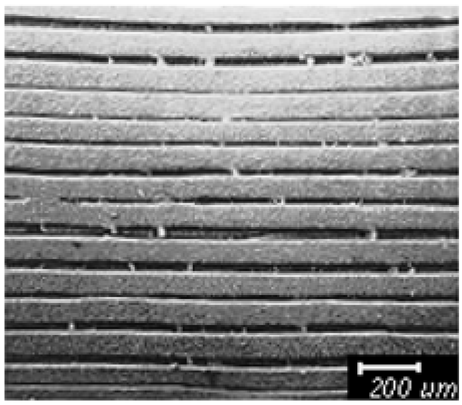

Fig. 1. Microstructure of Si_3N_4/BN-Al_2O_3 laminate.

*Corresponding author:
Tel : +82-55-751-5332
Fax: +82-55-755-6755
E-mail: dwshin@gsnu.ac.kr

Heat treatment at 260 °C for 2 h and at 400 °C for 4 h were used to remove the organic binder. Subsequently, the green body was hot pressed at 1800 °C for 1.5 h under a nitrogen atmosphere to give a laminated Si_3N_4. The microstructure of the laminated ceramics was examined using a SEM (CSM950, OPTON, Germany). Specimens were sliced into test bars (3 mm × 4 mm × 32 mm for bending strength and 4 mm × 6 mm × 32 mm for fracture toughness measurements). Flexural strength was measured with a span of 30 mm, and a crosshead speed of 0.5 mm/min at the room temperature. The fracture toughness was determined by the single-edge-notch-beam method at room temperature with a crosshead speed of 0.05 mm/minute.

Modeling of Laminated Structure

Laminate Structure

The microstructure of the synthesized Si_3N_4/BN-Al_2O_3 laminated ceramic is illustrate in Figure 1. The laminate contained two different parts: Si_3N_4 sheets having an average thickness of ~75 μm and a boundary phase of BN-Al_2O_3 having a thickness of 25 μm. The main layers and the interfaces are clearly seen to be separated (Fig. 1).

From the SEM observations, the structure of the laminates may be described as follows:

i) The laminated ceramic is built-up mainly of laminated sheets. The strength of these sheets is not the same everywhere but follows a Weibull distribution.

ii) These sheets which are separated by weak interfaces have the same structure and properties everywhere. The thickness and strength of the interface then is negligible.

Delamination Cracks

Two types of cracks exist during delamination under bending: breakthrough and interfacial. The breakthrough crack occurs in the main layers. When the driving force becomes more than the resistance force, a breakthrough crack is generated and propagates instantly for a length of one layer's thickness damaging one or more layers. According to the Griffith theory, the driving force is:

$$G_b = \frac{dW_b}{2bc} = \frac{\pi\sigma^2 c}{E} \tag{1}$$

where W_b is the interfacial strain energy, b is the specimen width, c is the length of the crack (thickness of one layer), E is Young's modulus, and σ is the stress loading on the layer. The resistance force can also be evaluated using Eq. (1) by the changing of σ to the average critical bending strength of the layers, σ_m.

The second type of crack is an interfacial crack which occurs only at the interface. The driving force of this crack is determined by the interfacial strain energy release rate, G_i :

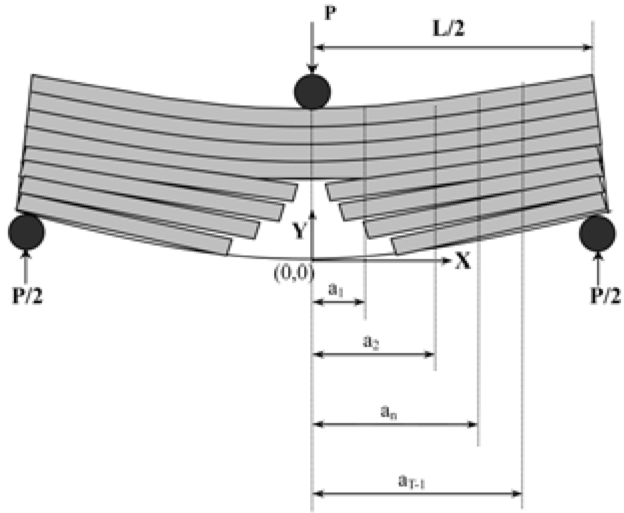

Fig. 2. Schematic illustration of a specimen under a three-point bending test, in which $\mathbf{a_n}$ is the length of nth interfacial crack.

$$G_i = \frac{P^2}{2b} \cdot \frac{dC}{da} \tag{2}$$

where P is the load, C is the specimen compliance, and α is the length of the interfacial crack. The resistance force is determined by the interfacial critical strain energy release rate, G_{ic}.

Analysis of the Fracture Process

The fracture process consists of two independent processes: the brittle collapse of the layer and the generation and propagation of interfacial cracks. In the case of the brittle collapsing layer, Figure 2 is a schematic illustrating the fracture process of a laminated ceramic. One breakthrough crack propagates for the length of one layer's thickness. For the next elementary fracture, another nearby layer gets damaged.

The other process is the generation and propagation of interfacial cracks. At the moment when a breakthrough crack expands, the loading is high enough for the generation of an interfacial crack in the interface layer, and the driving force is much higher than the resistance force ($G_i >> G_{ic}$), so the interfacial crack propagates rapidly even at constant roller displacement. Accompanying the generation and propagation of the interfacial crack, the elastic energy gets absorbed and the loading decreases rapidly, which creates a descending curve in the driving force. This process occurs instantly and ends at the equilibrium point G_i and G_{ic} [5].

Following this instantaneous process the loading again increases as the roller displacement increases. The driving force also increases, yet keeps a dynamic equilibrium with the resistance force. This leads to a steady propagation of the interfacial crack. This steady process continues until the loading increase is high enough to cause the next elementary fracture of the neighboring layer. The two fracture processes take place alternately until the material is completely broken into two pieces.

Mechanical Calculation of the Three-point Bend Test

A schematic of the specimen under the three-point bend test is shown in Fig. 2. It is assumed that break-through cracks occur only at the center of the beam and the interfacial cracks propagate symmetrically from the center. For the convenience of calculation, the zero of the coordinate is set at the bottom of the beam so that all the deformation becomes positive.

The loading, P, is evaluated from the expression :

$$P = U/C \tag{3}$$

where the U is the roller displacement and C is the specimen compliance.

Using the moment of inertia the beam, the maximum stress which occurs at the middle of the beam is:

$$\sigma_m = -\frac{MY}{I} = -\frac{PL}{2\cdot\frac{bH^3}{12}}(N-T)\left(\frac{\delta}{2}\right) \tag{4}$$

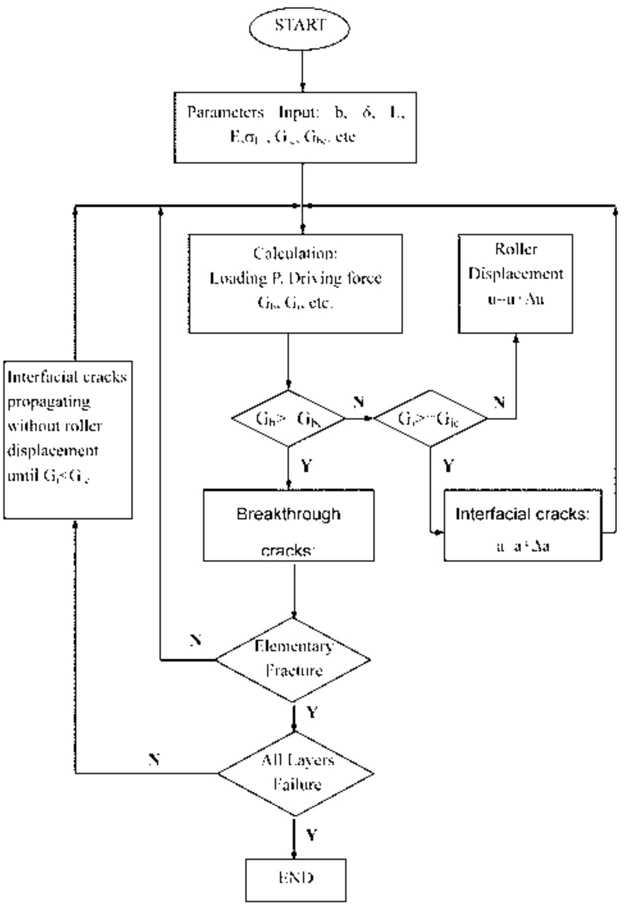

Fig. 3. Flow chart of a modeling calculation program.

where M is the bending moment, H is the height of the residual beam, b is the width of the beam, L is the loading span of the beam, δ is the thickness of one layer, N is the total number of layers, and T is the number of broken layers. Substituting these parameters into Eq. (1), the driving force of the breakthrough crack, G_b can be calculated.

The theoretical expression for the driving force for the interfacial cracks is dependent on G_i, which is [7] :

$$G_c = P^2(L-a_T)^2 f(N,b,\delta) \tag{5}$$

where α_T is the length of the interfacial crack which is indicated in Fig. 2 and f (N, b, δ) is a structural constant.

A flow chart is shown in Fig. 3 to illustrate the modeling simulation for the fracture procedure.

Comparison of the Model with Experimental Results

Simulation of the Fracture Process

The predicted load-displacement curve is presented in Fig. 4(a). The loading decreased sharply after every elementary fracture, then the interfacial cracks generated and propagated as the loading increased prior to the

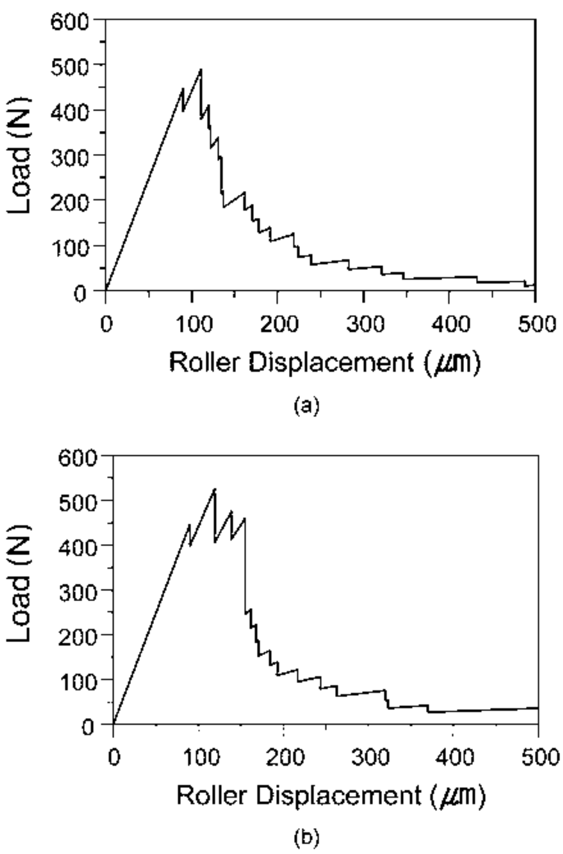

Fig. 4. Load-Displacement curve for laminated ceramics in three-point bending tests. Predicted by (a) modeling calculation (b) Experimental data.

next elementary fracture. For comparison with the experimental curve is shown in Fig. 4(b) which reflects the same tendency. This indicates that the prediction approximately mirrors the actual fracture process.

Energy Analysis and Fracture Toughness

The total work of the loading system is calculated from the area under the load-displacement curve. This includes the energy absorbed from crack propagation, strain energy, oscillatory energy, and sonic energy. The total work done per unit volume is given by :

$$W = \frac{\int_0^{u_{max}} Pdu}{2Nb\delta + 2b\sum_{i=1}^{T} a_i} \tag{6}$$

where W is the work of fracture which is often reported in research on laminated ceramics. The calculated result shows that W reaches a value of 6000 J/m^2.

A fundamental equation used to calculate the fracture toughness in solid mechanics is

$$K_I = \sqrt{\frac{EW}{1-\nu^2}} \tag{7}$$

where υ is the Poisson ratio of the solid considered.

Another important energy is the energy absorbed only for crack propagation which is the actual energy absorbed, W_{act}, and is defined by :

$$W_{act} = \frac{\sum_{i=1}^{T} a_n G_{ic} + N\delta G_{bc}}{2N\delta + 2\sum_{i=1}^{T} a_i} \tag{8}$$

where G_{bc} is the critical bulk strain energy release rate. The fracture toughness is :

$$K_I = \sqrt{\frac{EW_{act}}{1-\nu^2}} \tag{9}$$

Model Prediction

– Fracture toughness

Using Eq. (9), the fracture toughness of a standard specimen was calculated. The parameters used to predict the results on the basis of the proposed model are listed in Table 1. The value of the fracture toughness calculated using Eq. (9) is ~24 MPa·m$^{1/2}$ whereas the actual fracture toughness is 20 MPa·m$^{1/2}$ which shows that the model predicts the fracture toughness relatively accurately.

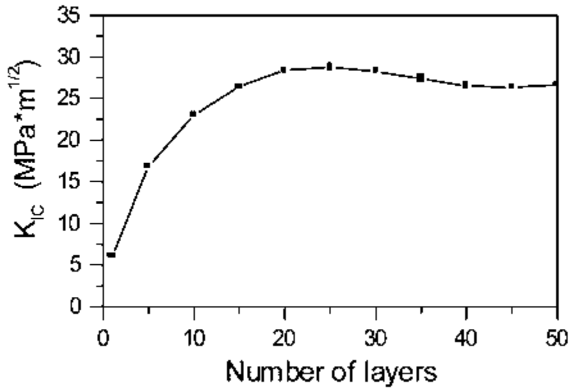

Fig. 5. Influence of layer thickness (number of layers in a standard specimen) on fracture toughness.

– Layer thickness

Figure 5 shows the influence of the layer thickness on the fracture toughness. As the number of layers in the standard specimen increases, the fracture toughness increases sharply until it reaches a maximum. Thereafter, the fracture toughness becomes almost constant, indicating that it is of no value to decrease the thickness of the layer indefinately in an attempt to make ceramics with still higher toughness ceramics.

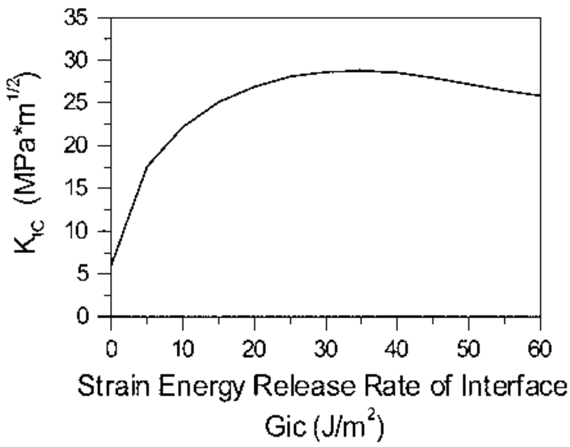

Fig. 6. Influence of the strain energy release rate of an interface (Gic) on toughness.

Table 1. Some Material parameter needed for calculation

Young's modulus E (GPa)	Bending strength of each layer σ_m(MPa)	Bulk strain energy release rate G_{bc} (J/m^2)	Interfacial strain energy release rate G_{bc} (J/m^2)	Number of layers	Thickness of each layer δ (mm)	Width of specimen b (mm)	Span L (mm)
310	651	113	10	30	0.1	4	15

– Interfacial properties

The influence of the interfacial properties such as the strain energy of the interface, G_{ic}, is shown in Fig. 6. The fracture toughness increases exponentially to a maximum and shows a slight decrease thereafter. This indicate that the interfacial toughness has a great affect on the fracture toughness of ceramics with weak interfaces.

Conclusions

A compact material with a laminated structure similar to nacre was successfully made. This laminated structure design provided a high fracture toughness for Si_3N_4/BN-Al_2O_3 laminated ceramic composites. A modified fracture process was proposed to describe the fracture behavior of a specimen experiencing three-point bending. The results demonstrate that the actual energy absorbed by crack propagation, W_{act} rather than the work-of-fracture was more suitable in order to calculate the toughness of composites. The layer thickness as well as the interfacial bonding strength influenced the properties of the laminated composites.

References

1. Z. Benlian. 5[10] (1995) 1261-1273.
2. Z. Benlian, JOM 4[2] (1994) 57-62.
3. X. Chunting and F. Jinghong, Mech. Res. 24[2] (1995) 220-231.
4. H. Liu and M.S. Hsu, J. Am. Ceram. Soc. 79[9] (1996) 2452-2457.
5. A.J. Phillipps, W.J. Clegg, and T.W. Clyne, Acta metall. Mater. 41[3] (1993) 805-817.
6. A.J. Phillipps, W.J. Clegg, and T.W. Clyne, Acta metall. Mater. 41[3] (1993) 819-827.
7. R.B. Pipes, R.A. Blake, and J.W. Gillespie, Delaware composites design encyclopedia, volume 4, Test methods, A Technomic Publishing Company, 126-132 (1990).